On Learning Hamiltonian Systems from Data*

Tom Bertalan

Massachusetts Institute of Technology tom@tombertalan.com

Igor Mezić

The University of California, Santa Barbara mezici@aimdyn.com

Felix Dietrich

Johns Hopkins University felix.dietrich@tum.de

Ioannis G. Kevrekidis

Johns Hopkins University yannisk@jhu.edu

Abstract

Concise, accurate descriptions of physical systems through their conserved quantities abound in the natural sciences. In data science, however, current research often focuses on regression problems, without routinely incorporating additional assumptions about the system that generated the data. Here, we propose to explore a particular type of underlying structure in the data: Hamiltonian systems, where an "energy" is conserved. Given a collection of observations of such a Hamiltonian system over time, we extract phase space coordinates and a Hamiltonian function of them that acts as the generator of the system dynamics. The approach employs an auto-encoder neural network component to estimate the transformation from observations to the phase space of a Hamiltonian system. An additional neural network component is used to approximate the Hamiltonian function on this constructed space, and the two components are trained simultaneously. As an alternative approach, we also demonstrate the use of Gaussian processes for the estimation of such a Hamiltonian. After two illustrative examples, we extract an underlying phase space as well as the generating Hamiltonian from a collection of movies of a pendulum. The approach is fully data-driven, and does not assume a particular form of the Hamiltonian function.

1 Introduction

Current data science exploration of dynamics often focuses on regression or classification problems, without routinely incorporating additional assumptions about the nature of the system that generated the data. This has started to change recently, with approaches to extract generic dynamical systems by [7], specifying the variables and possible expressions for the formulas beforehand. The Koopman operator and neural networks have also been employed to extract such generic expressions, conservation laws, or special group structures [4, 3]. In this paper, we propose to explore a particular type of underlying structure: data from Hamiltonian systems [1], where "energy" is conserved. The paper contains the following contributions:

1. Data-driven approximation (with two approaches: Gaussian processes and neural networks) of a Hamiltonian function on a given phase space, from time series data.

^{*}Submitted to NeurIPS on May 23, 2019. After submission of this paper, the paper at https://arxiv.org/abs/1906.01563 was uploaded to arXiv, where the authors address a related set of techniques.

- 2. Data-driven reconstruction of a phase space from (a) linear and (b) nonlinear transformations of the original Hamiltonian phase space.
- 3. A completely data-driven pipeline combining (a) the construction of an appropriate phase space and (b) the approximation of a Hamiltonian function on the new phase space, from nonlinear, high-dimensional observations (movies).

2 General description

A Hamiltonian system on Euclidean space $E = \mathbb{R}^{2n}$, $n \in \mathbb{N}$ is determined through a function $H: E \to \mathbb{R}$ that defines the equations

$$\dot{q}(t) = \partial H(q(t), p(t))/\partial p,$$
 (1)

$$\dot{p}(t) = -\partial H(q(t), p(t))/\partial q, \tag{2}$$

where () := d/dt, and $q(t), p(t) \in \mathbb{R}^n$ are interpreted as "position" and "momentum" coordinates in the "phase space" E. In many mechanical systems, and in all examples we discuss in this paper, the interpretation of the coordinates q, p is reflected in the dynamics through $\dot{q} = p$, i.e. $H(q, p) = \frac{1}{2}p^2 + h(q)$ for some function $h : \mathbb{R}^n \to \mathbb{R}^n$. In general, the equations (1, 2) imply that the Hamiltonian is constant along trajectories (q(t), p(t)), because

$$\frac{\mathrm{d}}{\mathrm{d}t}H(q(t),p(t)) = \frac{\partial H}{\partial q}(q(t),p(t)) \cdot \dot{q}(t) + \frac{\partial H}{\partial p}(q(t),p(t)) \cdot \dot{p}(t) = 0. \tag{3}$$

Equations (1, 2) can be restated as a partial differential equation for H at every $(q, p) \in E$:

$$\underbrace{\begin{bmatrix} 0 & I \\ -I & 0 \end{bmatrix}}_{Q} \cdot \nabla H(q, p) - \nu(q, p) = 0, \tag{4}$$

where $I \in \mathbb{R}^{n \times n}$ is the identity matrix and ν is the vector field on E (the left hand side of (1, 2)), which only depends on the position (q, p). The symplectic form on the given Euclidean space takes the form of the matrix ω .

In the next section, we discuss how to approximate the function H from given data points $D = \{(q_i, \dot{q}_i, \ddot{q}_i)\}_{i=1}^N$. This involves solving the partial differential Eqn. (4) for H. Since these equations determine H only up to an additive constant, we assume that we also know the value $H_0 = H(q_0, p_0)$ of H at a single point (q_0, p_0) in phase space. This is not a major restriction for the approach, because H_0 as well as (q_0, p_0) can be chosen arbitrarily.

3 Example: the nonlinear pendulum

As an example, consider the case n=1, and the Hamiltonian

$$H(q,p) = \frac{p^2}{2} + (1 - \cos(q)). \tag{5}$$

This Hamiltonian forms the basis for the differential equations of the nonlinear pendulum, $\ddot{q} = -\sin(q)$, or, in first-order form, $\dot{q} = \partial H(q,p)/\partial p = p$ and $\dot{p} = -\partial H(q,p)/\partial q = -\sin(q)$. In this section, we numerically solve PDE (4) by approximating the solution H using two approaches: Gaussian Processes [6] (§3.1) and neural networks (§3.2).

3.1 Approximation using Gaussian processes

We model the solution H as a Gaussian Process \hat{H} with a Gaussian covariance kernel,

$$k(x, x') = \exp(-\|x - x'\|^2 / \epsilon^2),$$
 (6)

where x and x' are points in the phase space, i.e. x=(q,p), x'=(q',p') and $\epsilon \in \mathbb{R}^+$ is the kernel bandwidth parameter. Given a collection X of N points in the phase space, as well as the function values H(X) at all points in X, the conditional expectation of the Gaussian Process \hat{H} at a new point y is

$$\hat{H}(y) = E[p(\hat{H}(y)|X)] = k(y,X)^T k(X,X')^{-1} H(X), \tag{7}$$

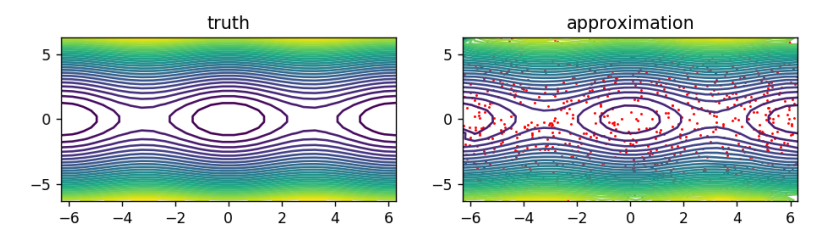


Figure 1: Solution using Gaussian Processes on a fine grid Y, with information about the derivative of H on a set of 625 randomly sampled points X (red points).

where we write $[k(X,X')]_{i,j} := k(x_i,x_j)$ for the kernel matrix evaluated over all x values in the given data set X. In Eqn. (7), the dimensions of the symbols are $y \in \mathbb{R}^{2n}$, $k(X,X') \in \mathbb{R}^{N \times N}$, $k(y,X) \in \mathbb{R}^N$, and $H(X) := (H(x_1),H(x_2),\ldots,H(x_N)) \in \mathbb{R}^N$. All vectors are column vectors. This illustrates that estimates of the solution H to the PDE at new points depend on the value of H over the entire data set. We do not know the values of H, but differentiating Eqn. (7) allows us to set up a system of equations to estimate H at points y from the information about the derivatives of H given by the time derivatives \dot{q} in Eqn. (1) and (the negative of) \dot{p} in Eqn. (2). Together with an arbitrary pinning term at a point x_0 , the list of known derivatives leads to the linear system of 2nN+1 equations,

$$\underbrace{\begin{bmatrix} \frac{\partial}{\partial x} k(x_1, Y)^T k(Y, Y')^{-1} \\ \frac{\partial}{\partial x} k(x_2, Y)^T k(Y, Y')^{-1} \\ \vdots \\ \frac{\partial}{\partial x} k(x_N, Y)^T k(Y, Y')^{-1} \\ k(x_0, Y)^T k(Y, Y')^{-1} \end{bmatrix}}_{\in \mathbb{R}^{(2nN+1) \times M}} \cdot \underbrace{[H(Y)]}_{\in \mathbb{R}^M} = \underbrace{\begin{bmatrix} g(X) \\ H_0 \end{bmatrix}}_{\mathbb{R}^{2nN+1}}, \tag{8}$$

where X is a data set of N points where we know the derivatives of H through $g(x_i) = (\frac{\partial H}{\partial q}(x_i), \frac{\partial H}{\partial p}(x_i))^T = (-\dot{p}_i, \dot{q}_i)^T \in \mathbb{R}^{2n}$. We evaluate on a fine grid Y of M points (such that $k(Y,Y') \in \mathbb{R}^{M \times M}, \frac{\partial}{\partial x} k(x_i,Y) \in \mathbb{R}^{2n \times M}$) and have information $g(X) \in \mathbb{R}^{2nN}$ on a relatively small set of N points called X (red dots in Fig. 1). The derivative of the Gaussian Process can be stated using the derivative of the kernel k with respect to the first argument. Solving this system of equations for H(Y) yields the approximation for the solution to the PDE (see Fig. 1). See [5] for a more detailed discussion of the solution of PDE with Gaussian Processes.

3.2 Approximation using an artificial neural network

Another possibility for learning the form of H using data is to represent the function with an artificial neural network (ANN) [2]. We write

$$\mathbf{x}_{l} = \sigma_{l}(\mathbf{x}_{l-1} \cdot \mathbf{W}_{l} + \mathbf{b}_{l}), \quad l = 1, \dots, L+1$$
(9)

where the activation function σ_l is nonlinear (for all the networks considered here, tanh) for $l=1,\ldots,L$ (if $L\geq 1$) and the identity for l=L+1. The learnable parameters of this ANN are $\{(\mathbf{W}_l,\mathbf{b}_l)\}_{l=1,\ldots,L+1}$, and we gather all such learnable parameters from the multiple layers that may be used in one experiment into a parameter vector w. If there are no hidden layers (L=0), then we learn an affine transformation $\mathbf{x}_1=\mathbf{x}_0\cdot\mathbf{W}+\mathbf{b}$. This format provides a surrogate function $\hat{H}(q,p)=x_{L+1}$, where the input x_0 is the row vector [q,p]. (Treating inputs as row vectors and using right-multiplication for weight matrices is convenient, as a whole batch of N inputs can be presented as an N-by-2 array.) Similarly, in the case(s) we need to learn additional transformations $\hat{\theta}$ and $\hat{\theta}^{-1}$ (see §4), they are also learned using such networks.

We collect training data by sampling a number of initial conditions in the rectangle $(q, p) \in [-2\pi, 2\pi] \times [-6, 6]$, then simulate short trajectories from each to provide a corpus of (q, p) points. For each of these, we additionally evaluate (\dot{q}, \dot{p}) . Shuffling over simulations once per

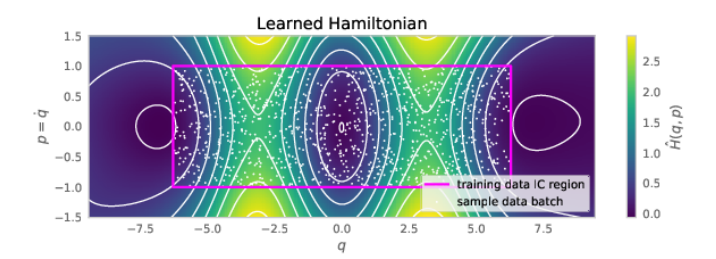


Figure 2: Learned Hamiltonian, with all loss terms included. Note that the learned function is only accurate where data sampling is sufficiently dense.

epoch, and dividing this dataset into batches, we then perform batchwise stochastic gradient descent to learn the parameters w using an Adam optimizer on the objective function defined below, with an exponentially decaying learning rate.

This objective function comprises a scalar function evaluated on each data 4-tuple $d = (q, p, \dot{q}, \dot{p})$ in the batch, and then averaged over the batch. This scalar function is written as

$$f(q, p, \dot{q}, \dot{p}; w) = \sum_{k=1}^{4} c_k f_k,$$
 (10)

$$f_{1} = \left(\frac{\partial \hat{H}}{\partial \hat{H}} - \dot{q}\right)^{2}, \qquad f_{2} = \left(\frac{\partial \hat{H}}{\partial \hat{H}} + \dot{p}\right)^{2},$$

$$f_{3} = \left(\hat{H}(q_{0}, p_{0}) - H_{0}\right)^{2}, \quad f_{4} = \left(\hat{H}\right)^{2} = \left(\frac{\partial \hat{H}}{\partial \hat{H}} \dot{q} + \frac{\partial \hat{H}}{\partial \hat{H}} \dot{p}\right)^{2},$$

$$(11)$$

where the dependence on w is through the learned Hamiltonian \hat{H} , the loss-term weights c_k are chosen to emphasize certain properties of the problem thus posed, and the partial derivatives of $\frac{\partial \hat{H}}{\partial \hat{H}}$ and $\frac{\partial \hat{H}}{\partial \hat{H}}$ are computed explicitly through automatic differentiation. Except for c_2 , all c_k values are set to either 1 or 0 depending on whether the associated loss term is to be included or excluded. Because of the square term in Eqn. (5), we set c_2 arbitrarily to 10 if nonzero, so the loss is not dominated by f_1 . An alternative might be to set c_1 to 1/10.

Since equations (1) and (2) together imply (3), any one of the three terms f_1 , f_2 , and f_4 could be dropped as redundant; therefore, we can set c_4 to zero, but monitor \hat{H} as a useful sanity check on the accuracy of the learned solution. In Fig. 2, we show the results of this process with our default nonzero values for c_k .

As an ablation study, we explored the effect (not shown here) of removing the first, second, and fourth terms. By construction, the true $H_t(q,p)$ function is zero for all (q,p). Note that this is only ever achieved to any degree in the central box, where data was densely sampled. Removing f_4 made no visible difference in the quality of our $\hat{H}_t \approx 0$ approximation, which was expected due to the redundancy in the set of equations (1), (2), and (3). However, removing either f_1 or f_2 gives poor results across the figure, despite the apparent redundancy of these terms with f_4 . This might be due to not balancing the contributions of the \dot{p} and \dot{q} terms, for which we attempted to compensate by unequal weighting values c_1 and c_2 .

4 Estimating Hamiltonian structure from observations

We now consider a set of observation functions $\theta: E \to \mathbb{R}^M$, $\theta=(y_1,\ldots,y_M)$, with $M \geq \dim E = n$, such that θ is a diffeomorphism between the phase space E and its image $\theta(E)$. In this setting, the notion of a symplectomorphism is important [1]. In general, a symplectomorphism is a diffeomorphism that leaves the symplectic structure on a manifold invariant. In our setting, a symplectomorphism of $E = Q \times P$ maps to a deformed space $\hat{E} = \hat{Q} \times \hat{P}$ where the system dynamics in the new variables $\hat{q} \in \hat{Q}$, $\hat{p} \in \hat{P}$ are conjugate to the original Hamiltonian dynamics (i.e., the push-forward of the original Hamiltonian function

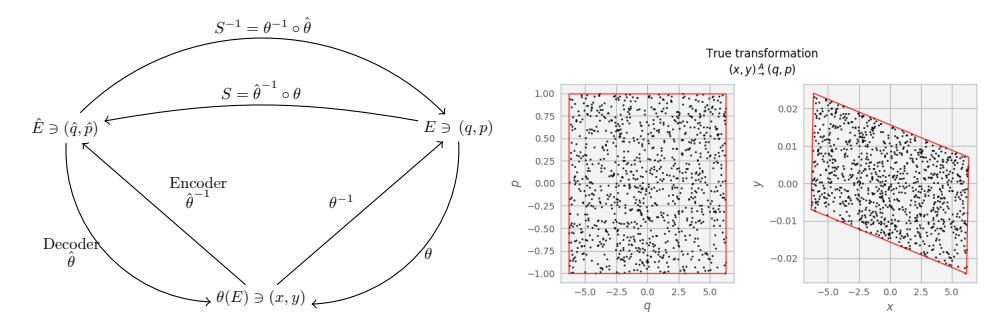


Figure 3: Left: Illustration of the network structure. Starting with observations of the (unknown) variables $(x,y) \in \theta(E)$, the autoencoder is structured to map via $\hat{\theta}^{-1}$ to the Hamiltonian form $(\hat{q}, \hat{p}) \in \hat{E}$ at left, as well as map back to the observations through $\hat{\theta}$. The complete process involves estimating a Hamiltonian for (the symplectomorphic copies of) p, q during training of the autoencoder. Right: The transformation θ from the original space q, p to the observed space x, y, for the linear example of §4.2.

onto \hat{q}, \hat{p} is the generator of the dynamics in these new coordinates). Not every diffeomorphism is a symplectomorphism, and we **do not assume** that θ is a symplectomorphism.

In the setting of this section, we do not assume access to E, H, or the explicit form of θ . Only a collection of points θ_i and time derivatives $\frac{d}{dt}\theta_i$ in the image $\theta(E)$ is available. We describe an approach to approximate a new map $\hat{\theta}^{-1}: \theta(E) \to \hat{E}$ into a symplectomorphic copy of E through an autoencoder [2], such that the transformed system in \hat{E} is conjugate to the original Hamiltonian system in E. Upon convergence, and if we had access to θ , the map $\hat{\theta}^{-1} \circ \theta \equiv S : E \to \hat{E}$ would approximate a symplectomorphism, and $\theta^{-1} \circ \hat{\theta} \equiv S^{-1}$ would be its inverse. During the estimation of $\hat{\theta}^{-1}$, we simultaneously approximate the new Hamiltonian function $\hat{H}: \hat{E} \to \mathbb{R}$. Fig. 3 visualizes the general approach, where only the information $(x,y)_i$ and $\frac{d}{dt}(x,y)_i$ is available to the procedure, while $\hat{\theta}^{-1}$ and a Hamiltonian \hat{H} on \hat{E} are constructed numerically.

4.1 A composite loss function for the joint learning of a transformation and a Hamiltonian

The following loss function is used to train an autoencoder component together with a Hamiltonian function approximation network component:

$$f(\hat{q}, \hat{p}, \dot{\hat{q}}, \dot{\hat{p}}; w) = \sum_{k} c_{k} f_{k},$$

$$f_{1} = \left(\frac{\partial \hat{H}}{\partial \hat{H}} - \dot{\hat{q}}\right)^{2}, \qquad f_{2} = \left(\frac{\partial \hat{H}}{\partial \hat{H}} + \dot{\hat{p}}\right)^{2},$$

$$f_{3} = \left(\hat{H}(\hat{\theta}^{-1}(x_{0}, y_{0})) - H_{0}\right)^{2}, \quad f_{4} = \left(\dot{\hat{H}}\right)^{2} = \left(\frac{\partial \hat{H}}{\partial \hat{H}} \dot{\hat{q}} + \frac{\partial \hat{H}}{\partial \hat{H}} \dot{\hat{p}}\right)^{2},$$

$$f_{5} = ||\hat{\theta}(\hat{\theta}^{-1}(x, y)) - [x, y]||^{2}, \quad f_{6} = \left(\det(D\hat{\theta}^{-1})\right)^{-2},$$

$$(12)$$

where the dependence on w is through the learned Hamiltonian \hat{H} and the learned transfor-

mations
$$\hat{\theta}$$
 and $\hat{\theta}^{-1}$, and the time derivatives in the space \hat{E} are computed as $\dot{\hat{q}} = \dot{x} \frac{\partial \hat{q}}{\partial \hat{q}} + \dot{y} \frac{\partial \hat{q}}{\partial \hat{q}}$ and $\dot{\hat{p}} = \dot{x} \frac{\partial \hat{p}}{\partial \hat{p}} + \dot{y} \frac{\partial \hat{p}}{\partial \hat{p}}$, using the Jacobian $D\hat{\theta}^{-1} = \begin{bmatrix} \frac{\partial \hat{q}}{\partial \hat{q}} & \frac{\partial \hat{q}}{\partial \hat{q}} \\ \frac{\partial \hat{p}}{\partial \hat{p}} & \frac{\partial \hat{q}}{\partial \hat{p}} \end{bmatrix}$ of the transformation $\hat{\theta}^{-1}$ (computed pointwise with automatic differentiation). When we learn an (especially nonlinear)

transformation $\hat{\theta}^{-1}$, in addition to the Hamiltonian $\hat{H}(\hat{q},\hat{p})$, including the f_4 term in the composite loss can have a detrimental effect on the learned transformation. There exists an easily-encountered naive local minimum in which $\hat{\theta}^{-1}$ maps all of the sampled values from

 $\theta(E) \ni (x,y)$ to a single point in \hat{E} , and the Hamiltonian learned is merely the constant function at the pinning value, $\hat{H}(\hat{q},\hat{p}) = \hat{H}_0$. In this state (or an approximation of this state), all of $\frac{\partial H}{\partial H}$, $\frac{\partial H}{\partial H}$, and the elements of $D\hat{\theta}^{-1}$ are zero, so the loss is zero (resp., small). A related failure is that in which the input in $\theta(E)$ is collapsed by $\hat{\theta}^{-1}$ to a line or curve in \hat{E} .

To alleviate both of these problems we added a new loss component f_6 . That is, we require that the learned transformation not collapse the input. It is sufficient for the corresponding weighting factor c_6 to be a very small nonzero value (e.g. 10^{-6}). The addition of f_6 to our loss helps us to avoid falling early in training into the unrecoverable local minimum described above, and also helps keep the scale of the transformed variables \hat{q} and \hat{p} macroscopic.

4.2 Example: linear transformation of the pendulum

We generate data from a rectangular region $x \in [-1,1], \ y \in [-1,1],$ then transform the region linearly with $\theta^{-1}(x,y) = A^{-1}[x,y]^T = [q,p]^T$. The matrix A^{-1} is the inverse of $A = R \cdot \Lambda$; a scaling followed by a rotation where $\Lambda = \begin{bmatrix} \lambda_1 & 0 \\ 0 & \lambda_2 \end{bmatrix}, \ \lambda_1 = 1, \ \lambda_2 = 64, \ R = \begin{bmatrix} \cos \rho & -\sin \rho \\ \sin \rho & \cos \rho \end{bmatrix}$, and $\rho = 5^\circ$. Our observation data $\theta(E)$ is thus given by $[x,y]^T = A \cdot [q,p]^T$. Using the true Hamiltonian $H(q,p) = p^2/2 + (1-\cos q)$, we additionally compute true values for dq/dt and dp/dt, and then use A to propagate these to x and y via $\frac{\mathrm{d}x}{\mathrm{d}t} = \frac{\partial x}{\partial q} \frac{\mathrm{d}q}{\mathrm{d}t} + \frac{\partial y}{\partial p} \frac{\mathrm{d}p}{\mathrm{d}t}$ and similar for y, where the partial derivatives are computed analytically (here, just the elements of A itself).

Our network is then presented with observation data x,y and its corresponding time-derivatives. Its task is to learn \hat{A} and \hat{A}^{-1} , which convert to and from variables \hat{q},\hat{p} (symplectomorphic to the original q,p); and a Hamiltonian \hat{H} in this new space. When evaluating the loss, the time derivatives of \hat{q} and \hat{p} are likewise computed via automatic differentiation using the chain rule through the learned transformation, e.g. as $\frac{\mathrm{d}\hat{q}}{\mathrm{d}t} = \frac{\partial \hat{q}}{\partial x} \frac{\mathrm{d}x}{\mathrm{d}t} + \frac{\partial \hat{q}}{\partial y} \frac{\mathrm{d}y}{\mathrm{d}t}$. Note also that $[\hat{q},\hat{p}]^T = \hat{A}^{-1} \cdot A \cdot [q,p]^T$, so if the original space E could be found, \hat{A} would satisfy $\hat{A} \cdot A^{-1} = I$. This cannot be expected given only the data in $\theta(E)$; we can only be sure that $\hat{A} \cdot A^{-1}$ approximates a symplectomorphism of the original E.

We could learn \hat{H} from a general class of nonlinear functions, as a small tanh neural network, but here we simply learn \hat{A} and \hat{A}^{-1} as linear transformations (that is, we have a linear "neural network", where L=0 in Eqn. (9), and \mathbf{b}_1 is constrained to be $\mathbf{0}$). As we include the reconstruction error of this autoencoder in our loss function, \hat{A}^{-1} is constrained to be the inverse of \hat{A} to a precision no worse than the f_1 and f_2 terms in Eqn. (12), after all three are scaled by their corresponding c_k values. In fact, for the linear case, initially the autoencoder's contribution to the loss is significantly lower than the Hamiltonian components (see Fig. 4), but, as training proceeds and the f_1 and f_2 terms are improved (at the initial expense of raising the autoencoder loss), larger reductions in loss are possible by optimizing \hat{H} rather than $\hat{\theta}$, so f_5 is decreased as quickly as (the larger of) f_1 or f_2 . That is, the autoencoder portion of the loss falls quickly to the level where it no longer contributes to the total loss given its weighting in the loss sum.

We find that the learned symplectomorphism $S(q,p) = \hat{A}^{-1} \cdot A \cdot [q,p]^T$, depicted in its q portion in Fig. 4, preserves q unmixed with p in one or the other of its two discovered coordinates. This is because both (a) $(q,p) \mapsto (p,-q)$ as well as (b) $(q,p) \mapsto (q,p+f(q))$ for any smooth function f are symplectomorphisms. They are special because $H(q,p) = \hat{H}(\hat{q}(q,p),\hat{p}(q,p))$, i.e. they even preserve the Hamiltonian. For the map (a), the transformation of the

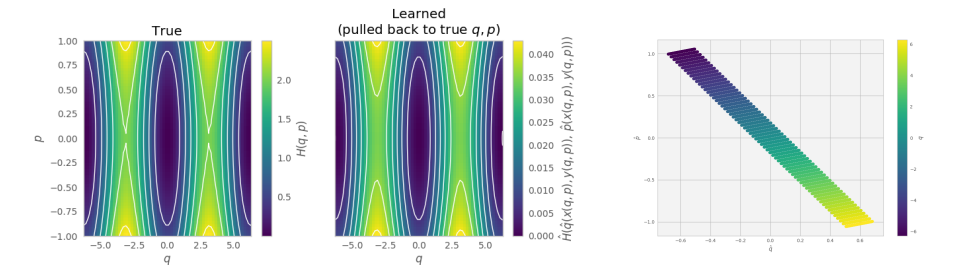


Figure 4: Learned $\hat{H}(\hat{q}, \hat{p})$ after a linear transformation θ . Left: The true function H(q,p) evaluated on a grid of q,p values. Center: The learned function on $\hat{q},\hat{p},$ pulled back onto the original q, p space. Right: learned linear symplectomorphism $S = \hat{\theta}^{-1} \circ \theta$.

Hamiltonian can be seen from the following derivation.

$$\dot{\hat{q}} = \dot{p} = -dH/dq = d\hat{H}/d\hat{p}, \tag{13}$$

$$\dot{\hat{p}} = -\dot{q} = -\mathrm{d}H/\mathrm{d}p = -\mathrm{d}\hat{H}/\mathrm{d}\hat{q},\tag{14}$$

$$d\hat{H}/dq = \partial\hat{H}/\partial\hat{q} \cdot \underbrace{d\hat{q}/dq}_{o} + \partial\hat{H}/\partial\hat{p} \cdot \underbrace{d\hat{p}/dq}_{i} = -\partial\hat{H}/\partial\hat{p} = dH/dq$$
 (15)

$$d\hat{H}/dq = \partial\hat{H}/\partial\hat{q} \cdot \underbrace{d\hat{q}/dq}_{=0} + \partial\hat{H}/\partial\hat{p} \cdot \underbrace{d\hat{p}/dq}_{=-1} = -\partial\hat{H}/\partial\hat{p} = dH/dq$$

$$d\hat{H}/dp = \partial\hat{H}/\partial\hat{q} \cdot \underbrace{d\hat{q}/dp}_{=1} + \partial\hat{H}/\partial\hat{p} \cdot \underbrace{d\hat{p}/dp}_{=0} = \partial\hat{H}/\partial\hat{q} = dH/dp.$$
(15)

Here, the first equality of (13, 14) follows from the map and the last equality of (13, 14) follows from the requirement that \hat{q}, \hat{p} follow Hamiltonian dynamics with respect to the new Hamiltonian \hat{H} . Equations (15,16) then show that the new Hamiltonian is the same as the old one (modulo a constant) when considered as a map on the old coordinates. A similar derivation can be made for the map (b). Note that arbitrary rotations of (q, p) are not symplectomorphisms.

Example: nonlinear transformation of the pendulum 4.3

In addition to the linear θ of §4.2, we show comparable results for a nonlinear transformation θ and learned $\hat{\theta}$. Specifically, we transform the data through $(x,y) = \theta(q,p)$ where

$$a = q/20$$
 $b = p/10$
 $x = a + (b + a^2)^2$ $y = b + a^2$, (17)

the inverse of which is given by $q = (x - y^2)20$ and $p = (y - x^2 + 2xy^2 - y^4)10$. We use the analytical Jacobian of this θ to compute the necessary \dot{x} and \dot{y} for input to our network.

We proceed as before, except that we no longer restrict the form of the learned $\hat{\theta}$ and $\hat{\theta}^{-1}$ to linear transformations, but instead allow small multi-layer perceptrons of a form similar to that used for \hat{H} .

The resulting learned symplectomorphism is again (in successfully converged runs) one which preserves a monotonically increasing or decreasing q in either \hat{q} or \hat{p} . This can be seen in Fig. 5.

Example: constructing a Hamiltonian system from nonlinear, high-dimensional observations of q, p

As a further demonstration of the method, we use a graphical rendering of the moving pendulum example from before as the transformation θ from the intrinsic state (q, p) to an image \mathbf{x} as our high-dimensional observable. We use a symplectic Euler's method to generate q(t), p(t) trajectories for various initial conditions, and then a simple custom renderer to display these as images (see Fig. 6). When rendering our video frames, we drag a tail of

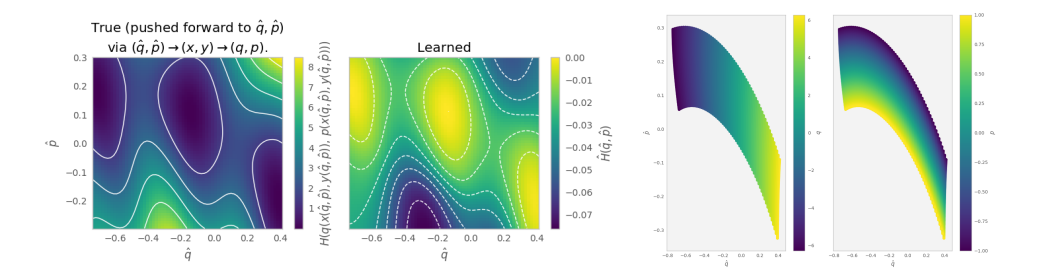


Figure 5: Results after a nonlinear transformation θ . Left: The true function H(q,p), pushed forward to \hat{q},\hat{p} . Center: The learned function on \hat{q},\hat{p} . A grid is now taken in \hat{E} , and transformed through S^{-1} for plotting H at corresponding q,p points. As is also true for the linear case, the sign of the learned \hat{H} may be flipped depending on whether we learn a representation of q via \hat{q} or \hat{p} which is monotonically increasing or decreasing. Right: Learned nonlinear symplectomorphism $S = \hat{\theta}^{-1} \circ \theta$. Again, we find that q is preserved (nearly) unmixed in the discovered space $\hat{E} \ni (\hat{q}, \hat{p})$.

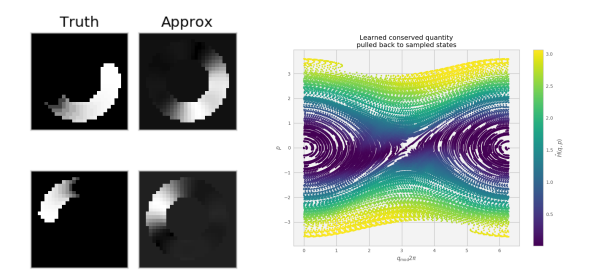


Figure 6: Left: PCA autoencoder reconstructions. The autoencoder is trained to reproduce PCA projections of the monochrome images on the left, where velocity p information is available in the length of the trail dragged behind the moving pendulum head. We show on the right these reconstructions passed back through the approximate inverse of the PCA projection. Note that only the magnitude of p is preserved. Right: Learned Hamiltonian. For each of the images \mathbf{x} in our dataset, we have an associated known q, p pair. Here, we plot these values, colored by the learned $\hat{H}(\mathbf{x})$.

decaying images behind the moving pendulum bob, so that information about both position q and velocity p is present in each rendered frame.

In order to make the approach agnostic to the data, we do not want to assume that the space \hat{E} is periodic, so instead, we use a four-dimensional phase space with elements $\hat{\mathbf{z}} = [\hat{q}_1, \hat{q}_2, \hat{p}_1, \hat{p}_2] = [\hat{\mathbf{q}}, \hat{\mathbf{p}}]$ and consider the splitting into (\hat{q}_1, \hat{q}_2) and (\hat{p}_1, \hat{p}_2) during training. In the space of input images, the manifold does not fill up four-dimensional space, but a cylinder, which is mapped to the four-dimensional encoding layer by the autoencoder.

In addition, to simplify the learning problem, we learn $\hat{\theta}^{-1}$ as the combination of a projection onto the first twenty principal components ψ followed by a dense autoencoder, reserving learning $\hat{\theta}^{-1}$ as an end-to-end convolutional autoencoder for future work. The encoding provides $\hat{\mathbf{z}}$ and, as before, we learn $\hat{\theta}^{-1}$ in tandem with \hat{H} , where now the conditions of Eqn. (12) are upgraded to vector equivalents to accommodate $\hat{\mathbf{z}}$.

In §4.1, we added a loss term proportional to the reciprocal of the determinant of the transformation's Jacobian in order to avoid transformations that collapsed the phase space. Here, this was not such an issue—of course, some collapsing of the high-dimensional representation is obviously required. Instead, a common mode of failure turned out to be learned constant \hat{H} functions, which automatically satisfy the Hamiltonian requirements (a constant is naturally a conserved quantity). To avoid this, we considered several possible ways to promote a

non-flat \hat{H} function, ultimately settling on (a) adding a term that encouraged the standard deviation of \hat{H} values to be nonzero, and (b) minimizing not just the mean squared error in our f_1 and f_2 terms, but also the max squared error, to avoid trivial bi-leveled $\hat{H}(q,p)$ functions.

The result, shown in Fig. 6, was a pulled-back $\hat{H}(q,p)$ function that at least in broad strokes resembles the truth, that satisfies $d\hat{H}/dt \approx 0$ (typically about 10^{-2}).

5 Conclusions

We described an approach to approximate Hamiltonian systems. It is a completely data-driven pipeline to (a) construct an appropriate phase space and (b) approximate a Hamiltonian function on the new phase space, from nonlinear, possibly high-dimensional observations (here, movies).

References

- [1] A. M. Almeida. *Hamiltonian systems: Chaos and quantization*. Cambridge University Press, 1992.
- [2] Ian Goodfellow, Yoshua Bengio, and Aaron Courville. *Deep Learning*. MIT Press, 2016. http://www.deeplearningbook.org.
- [3] Eurika Kaiser, J. Nathan Kutz, and Steven L. Brunton. Discovering conservation laws from data for control. In 2018 IEEE Conference on Decision and Control (CDC). IEEE, dec 2018.
- [4] Risi Kondor, Zhen Lin, and Shubhendu Trivedi. Clebsch-Gordan Nets: a Fully Fourier Space Spherical Convolutional Neural Network. In S. Bengio, H. Wallach, H. Larochelle, K. Grauman, N. Cesa-Bianchi, and R. Garnett, editors, Advances in Neural Information Processing Systems 31, pages 10117–10126. Curran Associates, Inc., 2018.
- [5] Maziar Raissi, Paris Perdikaris, and George Em Karniadakis. Inferring solutions of differential equations using noisy multi-fidelity data. *Journal of Computational Physics*, 335:736–746, apr 2017.
- [6] Carl Edward Rasmussen and Christopher K. I. Williams. Gaussian Processes for Machine Learning (Adaptive Computation And Machine Learning). The MIT Press, 2005.
- [7] Michael Schmidt and Hod Lipson. Distilling free-form natural laws from experimental data. *Science*, 324(5923):81–85, apr 2009.